Crack identification in rods and beams under uncertain boundary conditions

Michele Dilena[a], Marta Fedele Dell'Oste[a], Antonino Morassi[a,*],

[a] *Università degli Studi di Udine, Dipartimento Politecnico di Ingegneria e Architettura, via Cotonificio 114, 33100 Udine, Italy*

Abstract

This paper deals with the inverse problem of identifying a crack in a rod in axial vibration with partially unknown end conditions from a minimum number of resonant frequency variations. It is assumed that the crack is small and is modelled by an elastic spring acting along the rod axis. A first set of results concerns a uniform bar with both ends restrained by means of elastic springs having unknown flexibility. Under the hypothesis that the flexibility caused by the crack is small and of the same order of the flexibility of the elastic end constraints, it is shown that the inverse problem can be formulated in terms of the variations of the first three natural frequencies measured from the undamaged bar under ideal condition of fixed ends. It is proved that knowledge of this set of eigenfrequency variations can uniquely determine the overall flexibility induced by the end conditions, and the position (up to symmetry) and severity of the crack, by means of closed form expressions. The identification method can be also applied to axial vibrations of uniform cantilevers with elastically restrained end condition, and to transversely vibrating uniform beams either under elastic transverse support at both ends or under cantilever end conditions. The method was verified by numerical simulation and, in the case of the cantilever in bending vibration, by experimental data. Numerical analysis allowed to study in detail some singular situations occurring in the mathematical formulation of the inverse problem and to test the robustness of the method to errors on the data.

Keywords:
Crack, Identification, Unknown boundary conditions, Rods, Beams, Natural frequencies, Inverse problems

1. Introduction

In this paper we are concerned with the identification of a single open crack in a beam by natural frequency measurements. This topic has been the object of extensive research in the last three decades and, therefore, it is not easy to draw a complete bibliographic overview. Here, we limit ourselves to mention some of the contributions from which the interested reader can certainly obtain more information. Adams et al. wrote at the end of '70s the paper [1], which is considered the pioneering work on crack identification in beams from natural frequency data. They proved that, in case of localized and small damage, the ratio between the variation of two natural frequencies depends on the position of the damage only, not on its intensity. This property was subsequently extended by Hearn and Testa [10] and used for the implementation of a damage detection strategy in beam-like structures. Vestroni and Capecchi developed in a series of papers [23], [4], [24] a method for the identification of localized damage, such as cracks or notches, in beam structures based on the minimization of an objective function constructed with the differences between the experimental values of the natural frequencies and their counterparts obtained from a numerical model of the system. The procedure involves a first stage in which the damage is to be located, and a subsequent stage in which its intensity is estimated. Sinha et al. [22] proposed simplified models of cracked beams for which appropriate identification procedures mainly based on optimization problems were set. Khiem and Toan developed in [12] a method for the identification of multiple cracks in transversely vibrating uniform beams with clamped ends. The procedure is based on the so-called *crack scanning method*, recently proposed by the same authors, and on an improved Rayleigh's quotient type technique for calculating the crack induced changes in the natural frequencies. The detection of concentrated damage in more complex structures, such as parabolic arches or frames, by measured frequency variations has been approached in the papers by Pau et al. [17], [9]. Caddemi and Caliò [2], [3] have recently developed a multiple crack damage identification procedure in beams based on closed form solutions of the free vibration problem. The method makes use both of natural frequency data and pointwise mode shape information.

A closer analysis of the literature leads to the conclusion that most of the papers on damage identification in beam structures by frequency measurements are based on variational approach. This class of techniques allows one to deal with systems of high complexity (beams of variable profile under general set of end conditions, for example), but the approach has several drawbacks. They are mainly connected with the non-convexity of the error function and, as a consequence, with the appearance of several local and global minima. Basic questions such as how

*Corresponding author. Phone: (+39) 0432 558739; fax: (+39) 0432 558700

Email addresses: michele_dilena@email.it (Michele Dilena), martafedele@hotmail.com (Marta Fedele Dell'Oste), antonino.morassi@uniud.it (Antonino Morassi)

many natural frequency data are necessary to ensure uniqueness of the solution, at least in local sense, are rarely discussed in the literature and are mainly still open.

A different line of research was initiated by Narkis in the middle of '90s. In his paper [15], Narkis indicated certain conditions on a minimal set of measured natural frequencies which allow to determine *uniquely* the position of a *small* open crack in a uniform beam under axial or bending vibration with both ends free or pinned, respectively. Following Freund and Herrmann [8], the crack was modelled by means of a suitable elastic link connecting the two portions of beam adjacent to the damage. By linearizing the explicit expression of the characteristic equation of the damaged system in a neighborhood of the undamaged configuration, Narkis proved that the knowledge of the first order variation in the first two natural frequency induced by the crack can uniquely locate the crack by means of closed form expression. The result by Narkis was subsequently extended and generalized to other sets of end conditions by Morassi [14], who also obtained an explicit expression of the severity of the crack in terms of a suitable pair of natural frequencies. The perturbative approach used by Morassi was different from that of Narkis and, following Hearn and Testa [10], it was essentially based on the determination of an explicit expression of the first order derivative of the natural frequencies with respect to the damage severity in terms of quantities of the undamaged configuration of system. The uniqueness of the crack location in symmetric beams was resolved by Dilena and Morassi [6], who suggested to include appropriate anti-resonant frequency measurements in the input data.

The above-mentioned methods by Narkis [15], Morassi [14] and Dilena-Morassi [6] have been applied up to now to beams in axial or bending vibration under *ideal* boundary conditions, namely for beams with free, pinned or clamped ends. As far as we are aware, and despite the elastic constraints often represent a more realistic description of the boundary conditions of the real structural systems, studies on the identification of damage in beams with elastic constraints are rather rare. We refer, for example, to the contributions by Chondros and Dimarogonas [5], Ismail et al. [11], Sinha et al. [22]. In these works, the identification of damage - typically an open crack in a beam - is carried out separately from the determination of the elastic constants involved in the boundary condition description. Chondros and Dimarogonas [5] placed the crack exactly at the clamped end of a cantilever. Ismail et al. [11] estimated preliminarily the elastic support of a cantilever before proceeding to the identification of the damage. The same approach was followed by Sinha et al. [22]. The only paper that, at the best of our knowledge, contemplates simultaneously crack identification and boundary condition identification was authored by Narkis and Elmalah [16]. The authors considered a transversely vibrating uniform cantilever that, under operating conditions, shows a simultaneous flexibility of the clamped support and the occurrence of an open small crack in an interior cross-section. Under the assumption that the frequency variations caused by the weakening of the clamped end and that produced by the crack are small and of the same order, the authors showed that the crack position can be determined, without knowing exactly the boundary condition and the severity of damage, by measuring the variations in the first three natural frequencies of the cantilever.

In this paper we shall extend and generalize in several directions the results by Narkis and Elmalah. Our main goal is to determine a *minimal set* of natural frequency measurements that can guarantee the *unique* (where possible) determination of both the crack position and severity in the presence of elastic end supports with unknown stiffness. As in [16], we shall assume that the frequency variations produced by weakening the boundary conditions and those produced by the crack are small and of the same order. In Section 2.1 we shall consider the axial vibrations of a uniform beam with a single crack and with both ends elastically restrained with unknown stiffness. In Theorem 2.1 we shall show that knowledge of the variations in the first three natural frequencies allows to uniquely determine the position of the crack (up to symmetry) and its severity by means of closed form expressions. An extension of this result to the case of one free end and one elastically restrained end is presented in Theorem 2.2. The case of bending vibrations for a uniform beam with a small open crack and both ends supported by elastic constraints is considered in Section 2.2 (Theorem 2.3).

Our analysis is based on a suitable generalization of the crack identification method introduced in [14]. In the case of elastically restrained end conditions with unknown flexibility, however, the identification procedure becomes more involved than the case with ideal end conditions, and the analysis requires a new, specific treatment. One distinguish feature of our results is the determination of closed form expressions of the unknown parameters in terms of frequency variations. Another characteristic is the inability to estimate the flexibility of each end elastic constraint, since only the global support flexibility can be determined. Moreover, the analysis shows the presence of few singular situations in which one or more unknown quantities either cannot be identified or cannot be uniquely determined. These cases generally involve special positions of the crack and may have some relevance in the practical application of the method, as they may lead to inaccurate estimations of the unknown physical quantities. This is evidenced in the numerical and experimental simulations illustrated in Section 3.

2. Identification: Theory

2.1. Axial vibrations of rods

The infinitesimal, free, undamped longitudinal vibration of a thin uniform fixed-fixed rod, with radial frequency ω_n and amplitude $u_n = u_n(z)$, is governed by the eigenvalue problem

$$\begin{cases} EAu_n'' + \lambda_n \rho u_n = 0, \quad z \in (0, \ell) & (1) \\ u_n(0) = 0, & (2) \\ u_n(\ell) = 0. & (3) \end{cases}$$

Here, E is the Young's modulus of the material, A denotes the cross-sectional area, and ρ is the mass per unit length. The length of the rod is ℓ and $\lambda_n = \omega_n^2$ is the eigenvalue associated to the nth eigenfunction $u_n = u_n(z)$, $n \geq 1$. Hereinafter, $f'(z)$ denotes the first derivative of the function $f = f(z)$.

Problem (1)–(3) is considered as the *reference* eigenvalue problem of the supported rod. It is assumed that, during service, the rod is simultaneously affected by the degradation of the ideal constraint at the ends $z = 0$ and $z = \ell$, and by the occurrence of localized damage - a crack - at the cross-section of abscissa $z_d \in (0, \ell)$. The boundary condition at each end is modelled by means of an elastic spring reacting along the axis direction connecting each end to the fixed support. The end springs have stiffness $K_0 > 0$ at $z = 0$ and $K_\ell > 0$ at $z = \ell$. Following an approach commonly adopted in damage identification, the crack at z_d is assumed to remain open during vibration and it is modelled by inserting a translational elastic spring, of stiffness $K > 0$, at the damaged cross-section. The value of K can be expressed in terms of the geometry of the cracked cross-section and the properties of the material, see, for example, [8].

Under the above assumptions, the free longitudinal vibration of the cracked rod with elastically restrained ends (in brief, the *perturbed* rod) is governed by the eigenvalue problem

$$\begin{cases} EA\widetilde{u}_n'' + \widetilde{\lambda}_n \rho \widetilde{u}_n = 0, \quad z \in (0, z_d) \cup (z_d, \ell), & (4) \\ K_0 \widetilde{u}_n(0) = EA\widetilde{u}_n'(0), & (5) \\ K[[\widetilde{u}_n(z_d)]] = EA\widetilde{u}_n'(z_d), & (6) \\ [[\widetilde{u}_n'(z_d)]] = 0, & (7) \\ K_\ell \widetilde{u}_n(\ell) = -EA\widetilde{u}_n'(\ell), & (8) \end{cases}$$

where $(\widetilde{\lambda}_n, \widetilde{u}_n(z))$ is the nth perturbed eigenpair, $n \geq 1$, and $[[f(z_d)]] = \lim_{z \to z_d^+} f(z) - \lim_{z \to z_d^-} f(z)$. The eigenvalue problem (4)–(8) coincides with the reference problem (1)–(3) as, simultaneously, K_0, K_ℓ and K tend to infinity.

In this paper we shall consider rods in which the deviation of the end condition from the ideal case (e.g., perfect support) is small, namely the flexibility K_0^{-1}, K_ℓ^{-1} at both the end elastic supports is small and of the same order of smallness. Moreover, also the flexibility K^{-1} induced by the crack is assumed to be small, and of the same order of smallness of the support flexibility. Under the above assumptions, the inverse problem consists in determining the flexibility of the supports, the location and severity of the damage by measuring the variations in the first three natural frequencies of the rod from the reference to the perturbed configuration.

By adapting the perturbation approach proposed in [13], the first order change in the nth eigenvalue $\delta\lambda_n = \widetilde{\lambda}_n - \lambda_n$ is given by

$$\delta\lambda_n = -\frac{N_n^2(z_d)}{K} - \frac{N_n^2(0)}{K_0} - \frac{N_n^2(\ell)}{K_\ell}, \tag{9}$$

where

$$N_n(z) = EAu_n'(z), \quad z \in (0, \ell), \tag{10}$$

is the axial force associated to the nth eigenfunction of the unperturbed system, normalized as $\int_0^\ell \rho u_n^2(z)dz = 1$. A direct calculation shows that

$$\lambda_n = \frac{EA}{\rho\ell^2}(n\pi)^2, \quad u_n(z) = \sqrt{\frac{2}{\rho\ell}} \sin\left(n\pi\frac{z}{\ell}\right), \quad n \geq 1. \tag{11}$$

By writing (9) for $n = 1, 2, 3$ we obtain the following system of three nonlinear equations in the unknowns ξ, s and $\mathcal{F}$:

$$\begin{cases} C_1 = \xi \cos^2(\pi s) + \mathcal{F}, & (12) \\ C_2 = \xi \cos^2(2\pi s) + \mathcal{F}, & (13) \\ C_3 = \xi \cos^2(3\pi s) + \mathcal{F}, & (14) \end{cases}$$

where

$$\xi = \frac{EA/\ell}{K}, \quad \mathcal{F} = \frac{EA}{\ell}\left(\frac{1}{K_0} + \frac{1}{K_\ell}\right), \quad s = \frac{z_d}{\ell} \tag{15}$$

and

$$C_n = -\frac{\delta\lambda_n}{2\lambda_n}, \quad C_n > 0. \tag{16}$$

Two remarks on the system (12)–(14) are in order. First, the relative eigenvalue shifts $\frac{\delta\lambda_n}{\lambda_n}$ are equally affected by the end conditions and, in addition, the effect of the flexibility at the left and right end is not distinguishable by frequency measurements. Second, if $(s, \xi, \mathcal{F})$ is a solution to (12)–(14), then also $(1 - s, \xi, \mathcal{F})$ solves (12)–(14). This latter property is a consequence of the symmetry of the unperturbed configuration with respect to $z = \frac{\ell}{2}$, and it suggests to assume

$$s \in \left(0, \frac{1}{2}\right]. \tag{17}$$

Our first result is as follows.

Theorem 2.1. *The knowledge of $\{\delta\lambda_i\}_{i=1}^3$ determines uniquely the unknowns $s, \xi, \mathcal{F}$, with s satisfying* (17)*, by means of closed form expressions.*

The proof of Theorem 2.1 is based on two main steps. In Step 1, the system (12)–(14) is reduced to a second degree polynomial equation on a suitable trigonometric function of the damage location. In Step 2, a careful study of the solutions of this polynomial equation concludes the proof.

We start with Step 1. By introducing the auxiliary variable

$$x = \cos(2\pi s) \in [-1, 1), \tag{18}$$

system (12)–(14) becomes

$$\begin{cases} 2C_1 = \xi(1 + x) + 2\mathcal{F}, & (19) \\ C_2 = \xi x^2 + \mathcal{F}, & (20) \\ 2C_3 = \xi(2x - 1)^2(1 + x) + 2\mathcal{F}. & (21) \end{cases}$$

Combining the pair of equations (19)–(20) and (20)–(21), we can eliminate the unknown $\mathcal{F}$, obtaining the reduced system in the unknowns ξ and x:

$$\begin{cases} C_1 = \xi(2x + 1)(x - 1), & (22) \\ C_2 = \xi 4x(1 + x)(x - 1), & (23) \end{cases}$$

where

$$C_1 = 2(C_2 - C_1), \tag{24}$$

$$C_2 = 2(C_3 - C_1). \tag{25}$$

If $C_1 = 0$, then (22) gives $x = -\frac{1}{2}$, and the crack is uniquely localized at

$$s = \frac{1}{3}. \tag{26}$$

If $C_2 = 0$, then (23) gives either $x = 0$ or $x = -1$, and the crack is localized respectively at

$$s = \frac{1}{4} \quad \text{or} \quad s = \frac{1}{2}. \tag{27}$$

In both cases, the flexibilities ξ and $\mathcal{F}$ can be uniquely determined by (19)–(21). When $C_1 = 0$, the two equations (19), (20) are linearly dependent and it is necessary to include the third equation (21) in the analysis. By inserting $x = -\frac{1}{2}$ in (19) and (21), we obtain the linear system

$$\begin{cases} 2C_1 = \dfrac{\xi}{2} + 2\mathcal{F}, & (28) \\ 2C_3 = 2\xi + 2\mathcal{F}, & (29) \end{cases}$$

which has the unique solution

$$\xi = \frac{4}{3}(C_3 - C_1), \quad \mathcal{F} = \frac{4C_1 - C_3}{3}. \tag{30}$$

When $C_2 = 0$ and $x = 0$, from (19), (20) one finds

$$\xi = 2(C_1 - C_2), \quad \mathcal{F} = C_2. \tag{31}$$

Finally, if $C_2 = 0$ and $x = -1$, then

$$\xi = C_2 - C_1, \quad \mathcal{F} = C_1. \tag{32}$$

To complete the discussion of the *singular* cases, let us notice that conditions $C_1 = C_2 = 0$ can be also attained in the limit when s tends to 0^+ or, equivalently, when $x \to 1^-$. In fact, by continuity, equations (22) and (23) show that both C_1 and C_2 simultaneously tend to 0 as $x \to 1^-$, and equations (19)–(21) coincide, namely, $(\xi + \mathcal{F}) = C_1 = C_2 = C_3$. This means that the individual value of ξ and $\mathcal{F}$ remains unknown, and only the global flexibility $(\xi + \mathcal{F})$ can be determined when the crack approaches the support. We will see in the section of applications that this condition seriously affects the accuracy of the identification.

Suppose now that $C_1C_2 \neq 0$. Then, the ratio C_2/C_1 does not depend on ξ, e.g.,

$$\frac{C_2}{C_1} = \frac{4x(1+x)}{1+2x}, \tag{33}$$

and we obtain the following second degree polynomial equation in x:

$$4C_1x^2 + 2(-C_2 + 2C_1)x - C_2 = 0, \tag{34}$$

having the two distinct real solutions

$$x_1 = \frac{1}{4}\left(\left(\frac{C_2}{C_1} - 2\right) - \sqrt{4 + \left(\frac{C_2}{C_1}\right)^2}\right), \tag{35}$$

$$x_2 = \frac{1}{4}\left(\left(\frac{C_2}{C_1} - 2\right) + \sqrt{4 + \left(\frac{C_2}{C_1}\right)^2}\right), \tag{36}$$

with $x_1 < x_2$. Expressions (35), (36) suggest that the study of the ratio $\frac{C_2}{C_1}$ as a function of the damage location is useful in the present problem. It is convenient to rewrite C_1 and C_2 as functions of the new variable

$$t = \cos^2(\pi s), \quad t \in [0, 1), \tag{37}$$

namely

$$C_1(t) = 2\xi(1-t)(1-4t), \tag{38}$$

$$C_2(t) = 16\xi t(1-t)(1-2t). \tag{39}$$

The behavior of $C_1(t)$ and $C_2(t)$ is sketched in Figure 1 for $\xi > 0$, whereas the graph of the quotient

$$\frac{C_2(t)}{C_1(t)} = \frac{8t(1-2t)}{1-4t}, \quad t \in [0, 1), \tag{40}$$

is shown in Figure 2. By (35) and (36), it is easy to see that

$$\text{if } \frac{C_2}{C_1} < 0, \text{ then } x_1 < -1 \tag{41}$$

and

$$\text{if } \frac{C_2}{C_1} > \frac{8}{3}, \text{ then } x_2 > 1. \tag{42}$$

Therefore, in both cases only one solution of the pair $\{x_1, x_2\}$ is admissible, namely either x_2 or x_1 in case (41) or in case (42), respectively. In other words, if either $s \in \left(\frac{1}{4}, \frac{1}{3}\right)$ or $s \in \left(\frac{1}{3}, s^* = \frac{1}{\pi}\arccos\left(\frac{1}{\sqrt{6}}\right) \simeq 0.366\right)$, the position of the crack can be uniquely determined. At this stage, the flexibilities ξ and $\mathcal{F}$ can be evaluated uniquely using, e.g., (22) and, then, (19).

Let now examine the case in which the crack is located on the first quarter of the rod, e.g.,

$$s \in \left(0, \frac{1}{4}\right), \text{ that is } t = \cos^2(\pi s) \in \left(\frac{1}{2}, 1\right), \tag{43}$$

and let us try to determine the flexibility ξ of the damage by using equation (22):

$$C_1(t) = -\xi(1 + 2x_1(t(s)))(1 - x_1(t(s))), \tag{44}$$

where x_1 is given in (35). We want to show that the flexibility ξ in (44) turns out to be negative and, therefore, the solution x_1 is not admissible or, equivalently, the damage location is again determined uniquely in $\left(0, \frac{1}{4}\right)$ by using the second solution x_2. If $t \in \left(\frac{1}{2}, 1\right)$, then Figure 1(a) shows that $\frac{C_1(t)}{\xi} < 0$ in $\left(\frac{1}{2}, 1\right)$. Then, to find the contradiction it is enough to show that the right hand side of (44) is positive, that is (note that $1 - x_1 \geq 0$)

$$x_1(t) < -\frac{1}{2} \quad \text{when } t \in \left(\frac{1}{2}, 1\right). \tag{45}$$

Putting $\eta = \frac{C_2(t)}{C_1(t)}$, from Figure 2 we deduce that $\eta \in \left(0, \frac{8}{3}\right)$ when $t \in \left(\frac{1}{2}, 1\right)$, and it is easy to show that (45) leads to

$$\frac{1}{4}\left(\eta - 2 - \sqrt{4+\eta^2}\right) < -\frac{1}{2}, \tag{46}$$

that is

$$\eta < \sqrt{4+\eta^2}, \tag{47}$$

which is obviously always true. We conclude that (45) holds and, therefore, the left hand side of (44) is negative whereas the right hand side is positive, which is the desired contradiction.

Finally, the above discussion can be repeated to prove that also when

$$s \in \left(s^*, \frac{1}{2}\right), \tag{48}$$

the identification of the crack position is unique. In brief, condition (48) implies $t \in \left(0, \frac{1}{6}\right)$. Then, from Figure 2 we deduce that $\eta = \frac{C_2(t)}{C_1(t)} \in \left(0, \frac{8}{3}\right)$, and the solution x_1 leads to negative stiffness. The proof of Theorem 2.1 is complete.

The analysis presented above can be extended to include another set of end conditions, which is of importance in practical applications, namely the clamped-free rod or *cantilever*. Under the assumptions introduced at the beginning of this section, and using the same notation, the perturbed rod is elastically restrained (ER) at the left end at $z = 0$, whereas the right end, at $z = \ell$, is free. The longitudinal vibration of the cantilever with a crack of flexibility $\frac{1}{K}$ at $z = z_d$ is governed by an eigenvalue problem as in (4)–(8), with the exception of the end condition at $z = \ell$ which is replaced by the Neumann end condition

$$(\widetilde{u}_n^C)'(\ell) = 0. \tag{49}$$

Hereinafter, $(\widetilde{\lambda}_n^C, \widetilde{u}_n^C = \widetilde{u}_n^C(z))$ is the nth eigenpair of the perturbed rod, $n \geq 1$. The unperturbed eigenpairs have the explicit expression

$$\lambda_n^C = \frac{EA}{\rho\ell^2}\left(\frac{\pi}{2}(2n-1)\right)^2, \quad u_n^C(z) = \sqrt{\frac{2}{\rho\ell}}\sin\left(\frac{\pi}{2}(2n-1)\frac{z}{\ell}\right), \tag{50}$$

$n \geq 1$, and, as above, the flexibilities K_0^{-1}, K^{-1} are assumed to be small and of the same order of smallness. By writing (9) for $n = 1, 2, 3$, we obtain the nonlinear system

$$\begin{cases} C_1^C = \xi\cos^2(\frac{\pi}{2}s) + \mathcal{F}^C, & (51)\\ C_2^C = \xi\cos^2(\frac{3\pi}{2}s) + \mathcal{F}^C, & (52)\\ C_3^C = \xi\cos^2(\frac{5\pi}{2}s) + \mathcal{F}^C, & (53) \end{cases}$$

where ξ, s, $s \in (0,1)$, are as in (15) and

$$\mathcal{F}^C = \frac{EA}{\ell}\frac{1}{K_0}, \quad C_n^C = -\frac{\delta\lambda_n^C}{2\lambda_n^C}, \tag{54}$$

with $\delta\lambda_n^C = \widetilde{\lambda}_n^C - \lambda_n^C$, $n \geq 1$. In this case, it is convenient to introduce the position variable

$$x^C = \cos(\pi s) \in (-1, 1). \tag{55}$$

Then, system (51)–(53) takes the form

$$\begin{cases} 2C_1^C = \xi(1+x^C) + 2\mathcal{F}^C, & (56)\\ 2C_2^C = \xi(1+x^C)(2x^C-1)^2 + 2\mathcal{F}^C, & (57)\\ 2C_3^C = \xi(1+x^C)(1+2x^C-4(x^C)^2)^2 + 2\mathcal{F}^C. & (58) \end{cases}$$

Subtracting (56) from (57) and (58) side by side, we obtain

$$\begin{cases} C_1^C = \xi(1+x^C)((2x^C-1)^2-1), & (59)\\ C_2^C = \xi(1+x^C)((1+2x^C-4(x^C)^2)^2-1), & (60) \end{cases}$$

where we have defined the quantities C_1^C, C_2^C as

$$C_1^C = 2(C_2^C - C_1^C), \tag{61}$$

$$C_2^C = 2(C_3^C - C_1^C). \tag{62}$$

We distinguish two main cases, depending on the value of C_1^C. If $C_1^C = 0$, then by (59) and recalling that $x^C \in (-1,1)$, we have $x^C = 0$, and the crack is located at mid-span, e.g., $s = \frac{1}{2}$. Replacing $x^C = 0$ in (56)–(58), it is easy to see that only the "global" flexibility $(\xi + 2\mathcal{F})$ can be determined, e.g., $(\xi + 2\mathcal{F}) = 2C_1^C = 2C_2^C = 2C_3^C$, the individual values ξ and $\mathcal{F}$ being unknowns. Moreover, by repeating the analysis developed above for the ER rod, two additional singular cases with $C_1 = C_2 = 0$ occur as the crack approaches either the left ($s \to 0^+$, or $x^C \to 1^-$) or the right ($s \to 1^-$, or $x^C \to -1^+$) end of the rod. In the first case, we have $C_1^C = C_2^C = C_3^C = \xi + \mathcal{F}^C$ and the individual value of each flexibility remains unknown, whereas in the second case we obtain $C_1^C = C_2^C = C_3^C = \mathcal{F}^C$, and the estimate of ξ is missing. As before, it is expected that this indeterminacy will influence the numerical implementation of the identification method.

We shall now consider the case $C_1^C \neq 0$. Forming the quotient C_2^C/C_1^C, it turns out that the position variable x_1^C satisfies the second degree polynomial equation

$$(0 <)(x^C)^2 = \frac{1}{4} + \frac{C_2^C}{C_1^C}, \tag{63}$$

that is

$$x_1^C = -\sqrt{\frac{1}{4} + \frac{C_2^C}{C_1^C}}\ (<0), \quad x_2^C = \sqrt{\frac{1}{4} + \frac{C_2^C}{C_1^C}}\ (>0). \tag{64}$$

Now we shall prove that one of the two solutions (64) can always be excluded. To show this we insert the expression of C_1^C in (59), and we test it for $x^C = x_1^C$ and $x^C = x_2^C$. Recalling that $x^C \in (-1-1)$, it should be noticed that the factor $((2x^C-1)^2-1)$ on the right hand side of (59) takes positive or negative values when it is evaluated for $x^C = x_1^C$ or for $x^C = x_2^C$, respectively. Therefore, if $C_1^C < 0$, then the solution x_1^C should be excluded, since ξ must be a positive quantity. Similarly, when $C_1^C > 0$ then the solution x_2^C is discarded. In conclusion, only one solution of

the pair (64) remains and, since the function $x = x(s) = \cos(\pi s)$ is one-to-one from $(0, 1)$ into $(-1, 1)$, the crack is uniquely localized. Finally, the flexibility ξ of the crack can be determined uniquely using (59). Once s and ξ have been uniquely identified, also $\mathcal{F}^C$ can be uniquely determined.

In conclusion, we have proved the following result for the ER cracked cantilever.

Theorem 2.2. *The knowledge of $\{\delta\lambda_i^C\}_{i=1}^3$ determines uniquely the unknowns $s, \xi, \mathcal{F}^C$, for $s \in (0, 1) \setminus \{\frac{1}{2}\}$, by means of closed form expressions. If $s = \frac{1}{2}$, then the crack can be localized uniquely, but only the global flexibility $(\xi + 2\mathcal{F}^C)$ can be determined.*

2.2. Bending vibrations of beams

The first model that we shall consider is a uniform, thin, elastic Euler-Bernoulli beam under non-perfect end supports, and with an open crack at the cross-section of abscissa $z_d \in (0, \ell)$, where ℓ is the length of the beam. Each support of the beam is modelled by inserting a vertical elastic spring, acting transversally with respect to the beam axis, and with stiffness K_0 and K_ℓ at the end $z = 0$ and $z = \ell$, respectively. The crack is modelled by inserting a localized rotational spring of stiffness K at the cracked cross-section, see, for example, [8]. The infinitesimal, undamped, free bending vibration, of radian frequency $\sqrt{\widetilde{\mu}_n}$ and amplitude $\widetilde{v}_n = \widetilde{v}_n(z)$, is governed by the eigenvalue problem

$$\begin{cases} E\widetilde{I}\widetilde{v}_n'''' - \widetilde{\mu}_n\rho\widetilde{v}_n = 0, \quad z \in (0, z_d) \cup (z_d, \ell), & (65)\\ \widetilde{v}_n''(0) = 0, & (66)\\ K_0\widetilde{v}_n(0) = -E\widetilde{I}\widetilde{v}_n'''(0), & (67)\\ [[\widetilde{v}_n(z_d)]] = 0, & (68)\\ K[[\widetilde{v}_n'(z_d)]] = E\widetilde{I}\widetilde{v}_n''(z_d), & (69)\\ [[\widetilde{v}_n''(z_d)]] = 0, & (70)\\ [[\widetilde{v}_n'''(z_d)]] = 0, & (71)\\ K_\ell\widetilde{v}_n(\ell) = E\widetilde{I}\widetilde{v}_n'''(\ell), & (72)\\ \widetilde{v}_n''(\ell) = 0, & (73) \end{cases}$$

where E is the Young's modulus of the material, I is the moment of inertia of the cross-section, and ρ is the mass per unit length. The eigenpairs $\{\mu_n, v_n(z)\}_{n=1}^\infty$ of the *reference* beam, e.g., the beam simply supported at the ends and without damage, can be obtained as limit of the problem (65)–(73) as, simultaneously, K_0, K_ℓ and K tend to infinity. We have

$$\mu_n = \frac{EI}{\rho\ell^4}(n\pi)^4, \quad v_n(z) = \sqrt{\frac{2}{\rho\ell}}\sin\left(n\pi\frac{z}{\ell}\right), \quad n \geq 1. \qquad (74)$$

As in previous section, we assume that the elastically supported cracked beam is a perturbation of the reference beam, that is we assume K_0^{-1}, K_ℓ^{-1}, K^{-1} *small* and of the same order of smallness. Following [13], the first order change in the eigenvalue $\delta\mu_n$, $\delta\mu_n = \widetilde{\mu}_n - \mu_n$, induced by the damage and by the flexibility of the end conditions is given by

$$\delta\mu_n = -\frac{M_n^2(z_d)}{K} - \frac{T_n^2(0)}{K_0} - \frac{T_n^2(\ell)}{K_\ell}, \qquad (75)$$

where $M_n(z) = -EIv_n''(z)$, $T_n(z) = -EIv_n'''(z)$ is the bending moment and the shear associated to the normalized eigenfunction $v_n(z)$, respectively.

The diagnostic problem consists in determining the position and the severity of the crack, and the flexibility of the supports, by minimal eigenfrequency data. Replacing the expressions of $M_n(z)$ and $T_n(z)$ in (75), and writing this equation for $n = 1, 2, 3$, we obtain

$$\begin{cases} B_1 = \zeta\sin^2(\pi s) + \mathcal{G}, & (76)\\ B_2 = \zeta\sin^2(2\pi s) + 4\mathcal{G}, & (77)\\ B_3 = \zeta\sin^2(3\pi s) + 9\mathcal{G}, & (78) \end{cases}$$

where

$$\zeta = \frac{EI/\ell}{K}, \quad \mathcal{G} = \pi^2\frac{EI}{\ell^3}\left(\frac{1}{K_0} + \frac{1}{K_\ell}\right), \quad s = \frac{z_d}{\ell} \qquad (79)$$

and

$$B_n = -\frac{\delta\mu_n}{2\mu_n}, \quad B_n > 0. \qquad (80)$$

By the symmetry of the reference system, if $(s, \zeta, \mathcal{G})$ is a solution to (76)–(78), then also $(1-s, \zeta, \mathcal{G})$ solves (76)–(78). Therefore, in what follows we shall assume

$$s \in \left(0, \frac{1}{2}\right]. \qquad (81)$$

With the position variable

$$y = \cos(2\pi s) \in [-1, 1), \qquad (82)$$

the system (76)–(78) becomes

$$\begin{cases} 2B_1 = \zeta(1 - y) + 2\mathcal{G}, & (83)\\ B_2 = \zeta(1 - y^2) + 4\mathcal{G}, & (84)\\ 2B_3 = \zeta(1 - 4y^3 + 3y) + 18\mathcal{G}. & (85) \end{cases}$$

Using the first two equations (83)–(84) we can express $\mathcal{G}$ in terms of the remaining unknowns, and we obtain the reduced system

$$\begin{cases} \mathcal{B}_1 = \zeta(1 - y)^2, & (86)\\ \mathcal{B}_2 = 2\zeta(1 - y)^2(2 + y), & (87) \end{cases}$$

where

$$\mathcal{B}_1 = 4B_1 - B_2, \qquad (88)$$

$$\mathcal{B}_2 = 9B_1 - B_3. \qquad (89)$$

If either $\mathcal{B}_1 = 1$ or $\mathcal{B}_2 = 0$, then $y = 1$ and the crack is located at $s = 0$. Therefore, unknowns ζ and y disappear in equations (83)–(85), and only the global boundary flexibility $\mathcal{G}$ can be determined.

If, conversely, $y \neq 1$ then we can form the quotient $\mathcal{B}_2/\mathcal{B}_1$ and find

$$\frac{\mathcal{B}_2}{\mathcal{B}_1} = 2(2 + y), \qquad (90)$$

that is the unknown y is uniquely determined as

$$y = \frac{\mathcal{B}_2 - 4\mathcal{B}_1}{2\mathcal{B}_1}. \tag{91}$$

Since the function $y = y(s) = \cos(2\pi s)$ is one-to-one from $\left(0, \frac{1}{2}\right]$ to $[-1, 1)$, the position of the crack is uniquely determined in $\left(0, \frac{1}{2}\right]$. Once y is known, equations (83), (84) can be used, for example, to determine ζ and $\mathcal{G}$.

We have proved the following result.

Theorem 2.3. *The knowledge of $\{\delta\mu_i^C\}_{i=1}^3$ determines uniquely the unknowns $s, \zeta, \mathcal{G}$, for $s \in \left(0, \frac{1}{2}\right]$, by means of closed form expressions.*

We conclude the section by considering the inverse problem posed above for a cracked cantilever with non-perfect clamped end condition at the left end $z = 0$. We will see that the analysis of this case is more complicated and no closed form solutions are available.

Assume that the transverse displacement at $z = 0$ is hindered and the rotation of the end cross-section is contrasted by a rotational linearly elastic spring with stiffness K_0. The crack is modelled as above. The infinitesimal bending vibration of the perturbed cantilever is governed by the eigenvalue problem (65)–(73), in which the end conditions (66), (67) and (72), (73) at $z = 0$ and $z = \ell$, respectively, are replaced by

$$\widetilde{v}_n^C(0) = 0, \quad K_0(\widetilde{v}_n^C)'(0) = EI(\widetilde{v}_n^C)''(0), \tag{92}$$

$$(\widetilde{v}_n^C)''(\ell) = 0, \quad (\widetilde{v}_n^C)'''(\ell) = 0. \tag{93}$$

The eigenvalues of the perturbed and reference beam are denoted by $\{\widetilde{\mu}_n^C\}_{n=1}^\infty$ and $\{\mu_n^C\}_{n=1}^\infty$, respectively. Assuming K_0^{-1}, K^{-1} small and of the same order of smallness, the analysis in [13] shows that

$$\delta\mu_n = -\frac{(M_n^C(z_d))^2}{K} - \frac{(M_n^C(0))^2}{K_0}. \tag{94}$$

If $v_n^C = v_n^C(z)$ is an eigenfunction of the reference cantilever with the left end clamped and the right end free, then $M_n^C = M_n^C(z) = -EI(v_n^C)''(z)$ is an eigenfunction of the same cantilever with reversed end conditions. It follows that the end value $(M_n^C(0))^2$ can be expressed as

$$(M_n^C(0))^2 = 4\mu_n^C \frac{EI}{\ell}, \tag{95}$$

where the normalization condition $\int_0^\ell \rho(v_n^C(z))^2 dz = 1$ has been taken into account [18]. Writing (94) for $n = 1, 2, 3$ we obtain

$$\begin{cases} B_1' = \zeta \dfrac{(M_1^C(s))^2}{\mu_1^C} + 4\mathcal{G}', & (96) \\ B_2' = \zeta \dfrac{(M_2^C(s))^2}{\mu_2^C} + 4\mathcal{G}', & (97) \\ B_3' = \zeta \dfrac{(M_3^C(s))^2}{\mu_3^C} + 4\mathcal{G}', & (98) \end{cases}$$

where ζ and s are as in (79) and

$$B_n' = -\frac{\delta\mu_n^C}{\mu_n^C}, \quad \mathcal{G}' = \frac{EI}{\ell K_0}. \tag{99}$$

Subtracting (96) from (97) and from (98), and dividing the obtained equations side-by-side, the possible positions of the crack are the solutions of the equation

$$\frac{B_3' - B_1'}{B_2' - B_1'} = \frac{(M_3^C(s))^2(\mu_3^C)^{-1} - (M_1^C(s))^2(\mu_1^C)^{-1}}{(M_2^C(s))^2(\mu_2^C)^{-1} - (M_1^C(s))^2(\mu_1^C)^{-1}} \equiv f(s), \tag{100}$$

where $s \in (0, 1)$ and the difference $B_2' - B_1'$ is supposed not vanish. Equation (100) can be used to locate the crack for given (measured) value of the ratio $\frac{B_3' - B_1'}{B_2' - B_1'}$. In fact, the possible positions of the crack are the abscissae of the intersection points between the function $Y = f(s)$ and the straight line $Y = \frac{B_3' - B_1'}{B_2' - B_1'}$. The expression of the function $f(s)$ is *universal*, that is holds for all the uniform cantilevers of length ℓ. However, the study of the qualitative behavior of $f(s)$ it seems not easy to perform, since it involves the differences of the squared bending moments weighted with the inverse of eigenvalues. Postponing the general study of $f(s)$ to future work, in the section of applications we shall investigate on the numerical solutions of (100) in some specific cases.

3. Identification: Applications

In this section, numerical applications of the identification method are presented, both for longitudinal and bending vibrations. For the sake of simplicity, we shall consider a uniform rod or beam with unitary values of the physical parameters, i.e., $E = A = I = \ell = \rho = 1$. The identification problem is formulated by using pseudo-experimental frequency data, that is resonant frequencies are obtained by solving the direct eigenvalue problem in referential and perturbed configuration for different flexibilities of the support and different position and severity of the crack.

Simulations performed with noise-free data shall be presented in the next two subsections 3.1 and 3.2. It should be noticed, however, that even in these cases an intrinsic error is present on the frequency data, since the higher order terms on K^{-1}, K_0^{-1}, K_ℓ^{-1} are neglected in the first order Taylor series approximation (9).

To test the robustness of the method to errors on the data, in Subsection 3.3 the exact eigenvalue shift $\delta\lambda_n$ has been perturbed as follows

$$\delta\lambda_n^{err} = \delta\lambda_n(1 + \tau), \tag{101}$$

where τ is a Gaussian variable with vanishing mean and standard deviation σ given by $\sigma = \Pi/3$. Here, the number Π is the maximum error admitted on the eigenvalue shift, and simulations have been performed for values of Π equal to $0.05, 0.10, 0.20$, corresponding to errors up to 5%, 10%, 20%, respectively.

3.1. Axial vibrations of rods

The first series of simulations has been developed for the ER cracked rod (4)–(8). Figure 3 shows the results of identification varying the position s of the crack in the interval $\left(0, \frac{1}{2}\right]$ and for selected flexibility values ξ, $\mathcal{F}$ of the crack and of the elastic support, respectively. The flexibilities ξ and $\mathcal{F}$ have the same order of magnitude and each subfigure in Figure 3 shows three graphs corresponding to $\xi = 5 \cdot 10^{-3}$, $15 \cdot 10^{-3}$, $30 \cdot 10^{-3}$. The three columns of Figure 3 refer to results obtained for $\mathcal{F} = 5 \cdot 10^{-3}$, $15 \cdot 10^{-3}$, $30 \cdot 10^{-3}$, from the left to the right, respectively. The values of $\mathcal{F}$ correspond to relative eigenvalue shifts $\delta\lambda_n/\lambda_n$, $n = 1, 2, 3$, of about 1%, 3%, 5% of the unperturbed value, respectively, whereas the three levels of damage severity ξ cause relative eigenvalue shifts up to 1%, 3%, 5%, for the first three vibration modes. These percentage changes are typical of small levels of damage.

Identification errors on damage position are of order of few points per cent. The discrepancy increases as the crack approaches the support and as the severity of the damage increases. The determination of the flexibilities ξ and $\mathcal{F}$ is less accurate, with errors up to $10 - 15\%$ for damage location $s \in \left(\frac{1}{10}, \frac{1}{2}\right)$. When the crack is approaching the support, the estimates become very inaccurate and the identification of the flexibilities is seriously compromised. This behavior is a consequence of the singular conditions discussed in Section 2.1 and, specifically, it depends on the lack of estimates of the individual values of ξ and $\mathcal{F}$ when the crack is very closed to the elastic support. Numerical simulations suggest, however, that the accuracy improves as the flexibility $\mathcal{F}$ increases.

The second series of simulations concerns the cantilever rod analyzed in the second part of Section 2.1. Figure 4 shows the main results varying the position of the crack along the beam axis, and using the flexibility values $\mathcal{F}^C$, ξ as in previous Figure 3. The estimate of the crack position s turns out to be quite accurate, with percentage errors generally less then $5 - 6\%$. There are two exceptions. According with the analysis of the singular cases $s \to 0$ and $s \to 1$ of Theorem 2.2, the estimate of the crack position is not reliable in a neighborhood of the midpoint of the rod axis and a neighborhood of the free end of the rod. Within these regions and near the clamped end, numerical results show that the estimate of ξ is affected by large errors, which seem to prevent the use of the identification method in the intervals $\left(\frac{1}{2} - \frac{1}{10}, \frac{1}{2} + \frac{1}{10}\right)$, $\left(0, \frac{1}{10}\right)$ and $\left(\frac{8}{10}, 1\right)$, at least for the levels of damage considered here. Also the estimate of the boundary flexibility $\mathcal{F}^C$ is affected by this pathological behavior, although the accuracy of identification improves as the flexibility $\mathcal{F}^C$ increases.

3.2. Bending vibrations of beams

Identification for the elastically supported cracked beam (65)–(73) is discussed in this section. Due to the symmetry of the reference system, the results are presented in Figure 5 for crack belonging to the left half of the beam axis, i.e., $s \in \left(0, \frac{1}{2}\right]$. The global flexibility $\mathcal{G}$ of the supports has been chosen equal to $1 \cdot 10^{-4}$, $2 \cdot 10^{-4}$, $6 \cdot 10^{-4}$, corresponding to average percentage variation $\frac{\delta\lambda}{\lambda}$ of the first three eigenvalues of about 1%, 2%, 5% of the unperturbed values, respectively. The three levels chosen for the damage severity ζ, that is $\zeta = 5 \cdot 10^{-3}$, $15 \cdot 10^{-3}$, $30 \cdot 10^{-3}$, cause maximum percentage changes in the first three eigenvalues of about 1%, 2%, 5%, respectively.

Identification errors on damage position are small and of order of few points in the interval $\left(\frac{1}{10}, \frac{1}{2}\right)$ for values of the global boundary flexibility $\mathcal{G}$ equal to $1 \cdot 10^{-4}$ and $2 \cdot 10^{-4}$, whereas the estimates are less accurate in the interval $\left(0, \frac{1}{10}\right)$, see columns (a) and (b) in Figure 5. For $\mathcal{G} = 6 \cdot 10^{-4}$ a good agreement is found in a smaller interval $\left(\frac{3}{20}, \frac{1}{2}\right)$, see column (c) in Figure 5.

As already observed in the axial vibration cases, this behavior depends on the lack of estimates of the individual values of ζ and $\mathcal{G}$ when the crack is very closed to the elastic support. In addition, numerical simulations suggest that the accuracy improves as the ratio $\mathcal{G}/\zeta$ between the global and the internal flexibilities increases. As for the determination of $\mathcal{G}$ and ζ, the errors grow up to $30 - 40\%$ for the worst cases in the interval $\left(\frac{3}{20}, \frac{1}{2}\right)$. In the proximity of the beam supports the estimates are not accurate.

3.3. Sensitivity to errors

In presence of perturbations on the eigenvalues, 1000 simulations have been performed for each level of maximum error Π, as defined in Section 3. The results obtained for target values $s = 0.30$, $\xi = 5 \cdot 10^{-3}$ and $\mathcal{F} = \mathcal{F}^C = 5 \cdot 10^{-3}$, corresponding to small level of damage or boundary defect, are shown in Tables 1 and 2 for axial vibrations of rods under elastically supported and cantilever end conditions, respectively. It can be seen that the estimate of the crack position is accurate even for the maximum level of error $\Pi = 0.20$, with percentage deviations, defined as the ratio between the standard deviation and the average of the considered parameter, less than 6%. The identified values of the two flexibilities are more sensitive to errors, with deviations up to 18% and 8%, respectively for the internal spring and the elastic constraint, with $\Pi = 0.20$.

Table 3 shows the results of the identification for the elastically supported beam in bending vibration considered in Section 3.2. Target parameters are $s = 0.30$, $\zeta = 5 \cdot 10^{-3}$ and $\mathcal{G} = 1 \cdot 10^{-4}$. It is confirmed that the errors on the input data are not strongly amplified by the identification method, and the determination of the crack position is more stable than the estimates of the two flexibilities. As for the damage position, the percentage deviations are equal to 2%, 4%, 8% for maximum level of error $\Pi = 0.05, 0.10, 0.20$, respectively. The corresponding discrepancies for both the flexibilities are almost twice than previous values.

3.4. An experimental test

In this section we consider the cantilever in bending vibration analyzed in the second part of Section 2.2. The experimental results described in [16] are used to test the proposed identification technique. In that paper, the specimen consisted of a steel uniform beam having a rectangular cross section 30×3 mm and length 200 mm, see Figure 6. Young's modulus and density of mass were equal to 206000 MPa and 7800 kg/m^3, respectively. The beam was fixed at one end to a vibration device using two

tightening bolts. The non-perfect clamped condition was obtained by partially reducing the tightening torque in one bolt, whereas, to simulate an internal crack, a notch 0.1 mm wide and 0.2 mm deep was formed at a distance 40 mm ($s = 0.20$) from the fixed end. Dynamic tests were performed in the unperturbed and perturbed configurations; the first three frequencies were measured using an harmonic excitation, see Table 4.

The results of the identification are summarized in Table 5 and Figure 7. In particular, the graph of the function $f(s)$ defined in (100) and the horizontal straight line $Y = \frac{B'_3 - B'_1}{B'_2 - B'_1}$ are shown in Figure 7. The intersections between the curve and the line correspond to all the possible positions s_i of the crack satisfying the inverse problem (96)–(98). Once the positions are found, the flexibilities of the springs can be evaluated by means of equations (96) and (97). For the studied case, however, the solutions s_2 and s_3 can be discarded, since the corresponding values for the flexibility of the internal spring are negative, see Table 5. The remaining solution $s_1 = 0.22$ is closed to the effective position of the crack, with a relative error of about 2%. The result of identification coincides with the conclusions of the analysis developed in [16] (Section 4.2), even if we were unable to follow the arguments used by the authors to conclude that the solution of the inverse problem is unique without evaluating the values of the damage flexibility.

Finally, it can be observed from Figure 7 that the identification problem admits a unique solution for the position of the crack only in a narrow interval closed to the vertical asymptote $s = 0.364$.

4. Conclusions

Crack identification in beams can be developed by using changes in the resonant frequencies between an initial, referential state and a subsequent, damaged state. Results available in the literature mainly concern with the identification of the damage under the assumption that the boundary conditions are of ideal type (i.e., either free or perfectly fixed end conditions) and cannot change from the initial to the current configuration.

In this paper we have considered the identification of a single small open crack in a beam under elastically restrained end conditions of unknown flexibility. Under the assumption that the end flexibility is small and of the same order of the localized flexibility induced by the crack, a method was developed for the identification of the damage by using a minimum number of natural frequency information. Sufficient conditions allowing the unique solution of the inverse problem have been obtained in terms of the variations in the first three natural frequencies. Results have been obtained for initially uniform beams, either under axial or bending vibration, with different sets of elastically restrained end conditions. The location of the crack, its severity and the global flexibility induced by the end conditions have been determined, in most cases, by means of closed form expressions.

The method has been tested on an extended series of numerical simulations performed varying the position of the crack and for various values of the severity of the damage and flexibility of the end supports. A validation of the method on experimental data taken from [16] was also developed. Analytical results agree well with numerical and experimental tests.

Numerical simulations allowed to study in detail some singular situation, already emerged in the mathematical treatment of the inverse problem, in which one or more unknown quantities either cannot be identified or cannot be uniquely determined, even in presence of error free data. It can be shown that these pathological cases occur only for special positions of the crack, and are due to the truncation error in approximating the natural frequency variation by its first-order term in the Taylor's expansion (see, for example, (9)). Numerical results show that these cases may have some relevance in the practical application of the method since they may lead to inaccurate estimation of the unknown physical quantities. Generally, estimates of damage severity and boundary flexibility suffer from major errors when the crack is placed close to the ends of the beam. This suggests that the proposed method is accurate when the crack is far enough from the ends of the beam. The crack position estimate, on the contrary, is much less affected by these errors.

This error amplification had already partially emerged in the identification of two cracks in a simply supported uniform beam by natural frequency measurements of the bending vibration [20]. In that case, errors in crack severity estimates increase for close cracks placed near one end of the bar. Our analysis shows that in case of uncertain end conditions these effects are more important and could produce significant errors on the quantities to be identified. One way to reduce these unwanted effects would be to remove the hypothesis of small damage and work with generic severity of the crack by adapting the Lambda Curve Method proposed in [19]. In fact, this would avoid the introduction of truncation errors in the Taylor's series of the eigenvalues. The use of the Lambda Curve Method, however, is not trivial and, at present, its application to beams with elastically restrained end conditions is known only for bars in axial vibration with *known* boundary flexibility [7].

Finally, a possible extension of the proposed method is to the problem of identification of multiple small open cracks. It is likely that the method proposed recently by Shifrin [21] in the case of an initially uniform beam under ideal end conditions can be useful in this regard.

Acknowledgment

The authors gratefully acknowledge the financial support of the National Research Project PRIN 2015*TTJN*95 "Identification and monitoring of complex structural systems".

References

[1] R.D. Adams, P. Cawley, C.J. Pye, B.J. Stone, A vibration technique for non-destructively assessing the integrity of structures, *Journal of Mechanical Engineering Science* 20 (1978) 93–100.

[2] S. Caddemi, I. Caliò, The exact explicit dynamic stiffness matrix of multi-cracked Euler-Bernoulli beam and applications to damaged frame structures, *Journal of Sound and Vibration* 332 (2013) 3049–3063.

[3] S. Caddemi, I. Caliò, Exact reconstruction of multiple concentrated damages on beams, *Acta Mechanica* 225 (2014) 3137–3156.

[4] D. Capecchi, F. Vestroni, Monitoring of structural systems by using frequency data, *Earthquake Engineering and Structural Dynamics* 28 (2000) 447–461.

[5] T.G. Chondros, A.D. Dimarogonas, Identification of cracks in welded joints of complex structures, *Journal of Sound and Vibration* 69(4) (1980) 531–538.

[6] M. Dilena, A. Morassi, The use of antiresonances for crack detection in beams, *Journal of Sound and Vibration* 276 (2004) 195–214.

[7] J. Fernández-Sáez, A. Morassi, L. Rubio, Crack identification in elastically restrained vibrating rods, *International Journal of Non-Linear Mechanics* (in press) (2017); 10.1016/j.ijnonlinmec.2017.03.018.

[8] L.B. Freund, G. Herrmann, Dynamic fracture of a beam or plate in plane bending, *Journal of Applied Mechanics* 76-APM-15 (1976) 112–116.

[9] A. Greco, A. Pau, Damage identification in Euler frames, *Computer and Structures* 92-93 (2012) 328–336.

[10] G. Hearn, R.B. Testa, Modal analysis for damage detection in structures, *Journal of Structural Engineering ASCE* 117 (1991) 3042–3063.

[11] F. Ismail, A. Ibrahim, H.R. Martin, Identification of fatigue cracks from vibration testing, *Journal of Sound and Vibration* 140 (1990) 305-317.

[12] N.T. Khiem, L.K. Toan, A novel method for crack detection in beam-like structures by measurements of natural frequencies, *Journal of Sound and Vibration* 333 (2014) 4084-4103.

[13] A. Morassi, Crack-induced changes in eigenparameters of beam structures. *Journal of Mechanical Engineering ASCE* (1993) **119**:1798–1803.

[14] A. Morassi, Identification of a crack in a rod based on changes in a pair of natural frequencies, *Journal of Sound and Vibration* 242 (2001) 577–596.

[15] Y. Narkis, Identification of crack location in vibrating simply supported beams, *Journal of Sound and Vibration* 172 (1994) 549–558.

[16] Y. Narkis, E. Elmalah, Crack identification in a cantilever beam under uncertain end conditions. *International Journal of Mechanical Sciences* (1996) **38**:499–507.

[17] A. Pau, A. Greco, F. Vestroni, Numerical and experimental detection of concentrated damage in a parabolic arch by measured frequency variations, *Journal of Vibration and Control* 17(4) (2011) 605–614.

[18] J.W.S. Rayleigh, *The Theory of Sound*, Vol. 1, Dover Publications, New York, 1945.

[19] L. Rubio, J. Fernández-Sáez, A. Morassi, Identification of an open crack in a non-uniform rod by two frequency data, *International Journal of Solids and Structures* 75-76 (2015) 61–80.

[20] L. Rubio, J. Fernández-Sáez, A. Morassi, Identification of two cracks with different severity in beams and rods from minimal frequency data, *Journal of Vibration and Control* 22 (2016) 3102–3117.

[21] E.I. Shifrin, Identification of a finite number of small cracks in a rod using natural frequencies, *Mechanical Systems and Signal Processing* 70-71 (2016) 613-624.

[22] J.K. Sinha, M.I. Friswell, S. Edwards, Simplified models for the location of cracks in beam structures using measured vibration data, *Journal of Sound and Vibration* 251 (2002) 13-38.

[23] F. Vestroni, D. Capecchi, Damage evaluation in cracked vibrating beams using experimental frequencies and finite element model, *Journal of Vibration and Control* 2(1) (1996) 69–86.

[24] F. Vestroni, D. Capecchi, Damage detection in beam structures based on frequency measurements, *Journal of Engineering Mechanics ASCE* 126 (2000) 761-768.

Table Captions

Table 1. Results of identification for the cracked rod $E = A = \ell = \rho = 1$ with elastically restrained ends (4)–(8) and with noisy data as in (101). Unknown parameters: $s = 0.30$, $\xi = 5 \cdot 10^{-3}$, $\mathcal{F} = 5 \cdot 10^{-3}$. Percentage errors: $err_s = 100 \times (s_{average} - s_{exact})/\ell$, $err_\xi = 100 \times (\xi_{average} - \xi_{exact})/\xi_{exact}$ and $err_\mathcal{F} = 100 \times (\mathcal{F}_{average} - \mathcal{F}_{exact})/\mathcal{F}_{exact}$.

Table 2. Results of identification for the cracked rod $E = A = \ell = \rho = 1$ under cantilever end conditions and with noisy data as in (101). Unknown parameters: $s = 0.30$, $\xi = 5 \cdot 10^{-3}$, $\mathcal{F} = 5 \cdot 10^{-3}$. Percentage errors: $err_s = 100 \times (s_{average} - s_{exact})/\ell$, $err_\xi = 100 \times (\xi_{average} - \xi_{exact})/\xi_{exact}$ and $err_{\mathcal{F}^C} = 100 \times ({\mathcal{F}^C}_{average} - {\mathcal{F}^C}_{exact})/{\mathcal{F}^C}_{exact}$.

Table 3. Results of identification for the transversely vibrating beam $E = I = \ell = \rho = 1$ with elastic supports (65)–(73) and with noisy data as in (101). Unknown parameters: $s = 0.30$, $\zeta = 5 \cdot 10^{-3}$, $\mathcal{G} = 1 \cdot 10^{-4}$. Percentage errors: $err_s = 100 \times (s_{average} - s_{exact})/\ell$, $err_\zeta = 100 \times (\zeta_{average} - \zeta_{exact})/\zeta_{exact}$ and $err_\mathcal{G} = 100 \times (\mathcal{G}_{average} - \mathcal{G}_{exact})/\mathcal{G}_{exact}$.

Table 4. Experimental natural frequencies and their relative variations between undamaged and damaged configurations. Data taken from [16]. Frequency variations: $\Delta f = 100 \times (f_{\mathrm{Und}} - f_{\mathrm{Dam}})/f_{\mathrm{Und}}$.

Table 5. Results of damage identification for the cantilever in bending vibration. Actual damage location: $z_d = 40$ mm.

Figure Captions

Figure 1. Graph of the functions $C_1(t)$ and $C_2(t)$ defined in equations (38) and (39), respectively.

Figure 2. Graph of the function $\frac{C_2(t)}{C_1(t)}$ defined in equation (40).

Figure 3. Elastically restrained cracked rod (4)–(8): identification using the variations of the first three eigenfrequencies of the longitudinal vibration. Values of $\mathcal{F}$: $\mathcal{F} = 5 \cdot 10^{-3}$ (left column), $\mathcal{F} = 15 \cdot 10^{-3}$ (central column), $\mathcal{F} = 30 \cdot 10^{-3}$ (right column). Percentage errors: $err(s) = 100 \times (s_{ident} - s_{exact})/\ell$, $err(\xi) = 100 \times (\xi_{ident} - \xi_{exact})/\xi_{exact}$, $err(\mathcal{F}) = 100 \times (\mathcal{F}_{ident} - \mathcal{F}_{exact})/\mathcal{F}_{exact}$.

Figure 4. Elastically restrained cracked cantilever: identification using the variations of the first three eigenfrequencies of the longitudinal vibration. Values of $\mathcal{F}^C$: $\mathcal{F}^C = 5 \cdot 10^{-3}$ (left column), $\mathcal{F}^C = 15 \cdot 10^{-3}$ (central column), $\mathcal{F}^C = 30 \cdot 10^{-3}$ (right column). Percentage errors: $err(s) = 100 \times (s_{ident} - s_{exact})/\ell$, $err(\xi) = 100 \times (\xi_{ident} - \xi_{exact})/\xi_{exact}$, $err(\mathcal{F}^C) = 100 \times (\mathcal{F}^C{}_{ident} - \mathcal{F}^C{}_{exact})/\mathcal{F}^C{}_{exact}$.

Figure 5. Elastically supported cracked beam (65)–(73): identification using the variations of the first three eigenfrequencies of the bending vibration. Values of $\mathcal{G}$: $\mathcal{G} = 1 \cdot 10^{-4}$ (left column), $\mathcal{G} = 2 \cdot 10^{-4}$ (central column), $\mathcal{G} = 6 \cdot 10^{-4}$ (right column). Percentage errors: $err(s) = 100 \times (s_{ident} - s_{exact})/\ell$, $err(\zeta) = 100 \times (\zeta_{ident} - \zeta_{exact})/\zeta_{exact}$, $err(\mathcal{G}) = 100 \times (\mathcal{G}_{ident} - \mathcal{G}_{exact})/\mathcal{G}_{exact}$.

Figure 6. The cracked cantilever in bending vibration considered in [16]. (a) Schematic illustration of the experimental setup; (b) mechanical model; (c) cracked cross-section. Length in mm.

Figure 7. Results of damage identification for the cantilever in bending vibration. Actual damage location: $s = 0.20$.

Table 1: Results of identification for the cracked rod $E = A = \ell = \rho = 1$ with elastically restrained ends (4)–(8) and with noisy data as in (101). Unknown parameters: $s = 0.30, \xi = 5{\cdot}10^{-3}, \mathcal{F} = 5{\cdot}10^{-3}$. Percentage errors: $err_s = 100\times(s_{average}-s_{exact})/\ell$, $err_\xi = 100\times(\xi_{average}-\xi_{exact})/\xi_{exact}$ and $err_\mathcal{F} = 100\times(\mathcal{F}_{average}-\mathcal{F}_{exact})/\mathcal{F}_{exact}$.

	$\Pi = 0.05$			$\Pi = 0.10$			$\Pi = 0.20$		
Stat. Property	s	ξ	$\mathcal{F}$	s	ξ	$\mathcal{F}$	s	ξ	$\mathcal{F}$
max	0.314	0.00563	0.00524	0.324	0.00632	0.00558	0.349	0.00792	0.00627
min	0.290	0.00412	0.00457	0.277	0.00353	0.00430	0.249	0.00196	0.00362
average	0.301	0.00492	0.00496	0.301	0.00496	0.00494	0.301	0.00502	0.00492
error (%)	0.3	−1.6	−0.8	0.3	−0.8	−1.2	0.3	0.4	−1.6
std dev	0.004	0.00023	0.00010	0.007	0.00045	0.00019	0.015	0.00087	0.00039

Table 2: Results of identification for the cracked rod $E = A = \ell = \rho = 1$ under cantilever end conditions and with noisy data as in (101). Unknown parameters: $s = 0.30$, $\xi = 5 \cdot 10^{-3}$, $\mathcal{F} = 5 \cdot 10^{-3}$. Percentage errors: $err_s = 100 \times (s_{average} - s_{exact})/\ell$, $err_\xi = 100 \times (\xi_{average} - \xi_{exact})/\xi_{exact}$ and $err_{\mathcal{F}^C} = 100 \times ({\mathcal{F}^C}_{average} - {\mathcal{F}^C}_{exact})/{\mathcal{F}^C}_{exact}$.

	$\Pi = 0.05$			$\Pi = 0.10$			$\Pi = 0.20$		
Stat. Property	s	ξ	$\mathcal{F}^C$	s	ξ	$\mathcal{F}^C$	s	ξ	$\mathcal{F}^C$
max	0.320	0.00557	0.00523	0.336	0.00633	0.00558	0.422	0.00788	0.00599
min	0.292	0.00416	0.00471	0.282	0.00343	0.00445	0.264	0.00230	0.00385
average	0.304	0.00489	0.00496	0.305	0.00486	0.00497	0.305	0.00496	0.00494
error (%)	1.3	−2.2	−0.8	1.7	−2.8	−0.6	1.7	−0.8	−1.2
std dev	0.004	0.00022	0.00009	0.008	0.00044	0.00017	0.017	0.00087	0.00034

Table 3: Results of identification for the transversely vibrating beam $E = I = \ell = \rho = 1$ with elastic supports (65)–(73) and with noisy data as in (101). Unknown parameters: $s = 0.30$, $\zeta = 5 \cdot 10^{-3}$, $\mathcal{G} = 1 \cdot 10^{-4}$. Percentage errors: $err_s = 100 \times (s_{average} - s_{exact})/\ell$, $err_\zeta = 100 \times (\zeta_{average} - \zeta_{exact})/\zeta_{exact}$ and $err_\mathcal{G} = 100 \times (\mathcal{G}_{average} - \mathcal{G}_{exact})/\mathcal{G}_{exact}$.

	$\Pi = 0.05$			$\Pi = 0.10$			$\Pi = 0.20$		
Stat. Property	s	ζ	$\mathcal{G}$	s	ζ	$\mathcal{G}$	s	ζ	$\mathcal{G}$
max	0.320	0.00540	0.000110	0.337	0.00613	0.000116	0.368	0.01018	0.000126
min	0.282	0.00446	0.000088	0.263	0.00412	0.000074	0.209	0.00359	0.000007
average	0.303	0.00488	0.000100	0.302	0.00493	0.000099	0.301	0.00503	0.000097
error (%)	1.0	−2.4	0.0	0.7	−1.4	−1.0	0.3	0.6	−3.0
std dev	0.006	0.00014	0.000003	0.011	0.00029	0.000006	0.023	0.00069	0.000014

Table 4: Experimental natural frequencies and their relative variations between undamaged and damaged configurations. Data taken from [16]. Frequency variations: $\Delta f = 100 \times (f_{\text{Und}} - f_{\text{Dam}})/f_{\text{Und}}$.

Mode	Undamaged	Damaged	
	[Hz]	[Hz]	Δf [%]
1	56.63	55.21	2.5
2	358.10	350.00	2.3
3	1015.60	991.40	2.4

Table 5: Results of damage identification for the cantilever in bending vibration. Actual damage location: z_d = 40 mm.

Solution	$s = z_d/L$	z_d [mm]	ζ	K [N m]	$\mathcal{G}$'	K_0 [N m]
1	0.2217	44.3	0.00248	28613	0.01118	6339
2	0.3865	77.3	-0.01395	-5081	0.01557	4552
3	0.5974	119.5	-0.00288	-24635	0.01254	5652

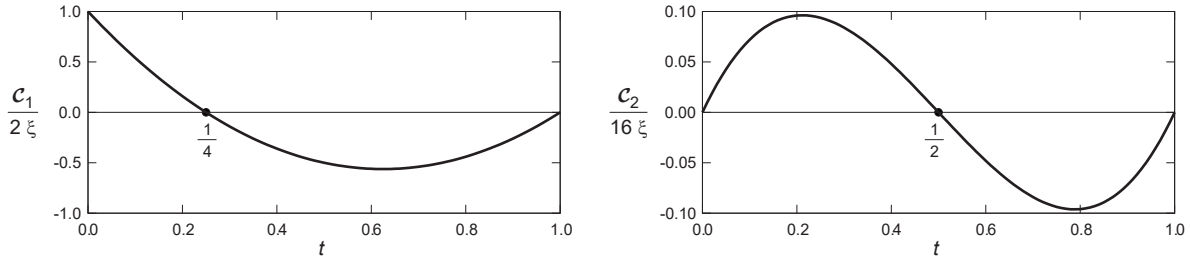

Figure 1: Graph of the functions $C_1(t)$ and $C_2(t)$ defined in equations (38) and (39), respectively.

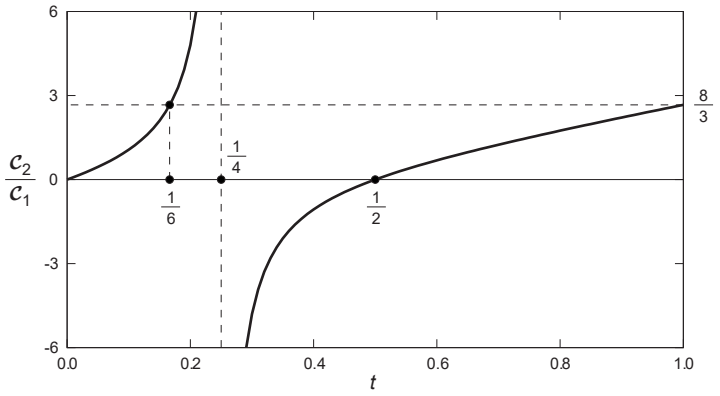

Figure 2: Graph of the function $\frac{C_2(t)}{C_1(t)}$ defined in equation (40).

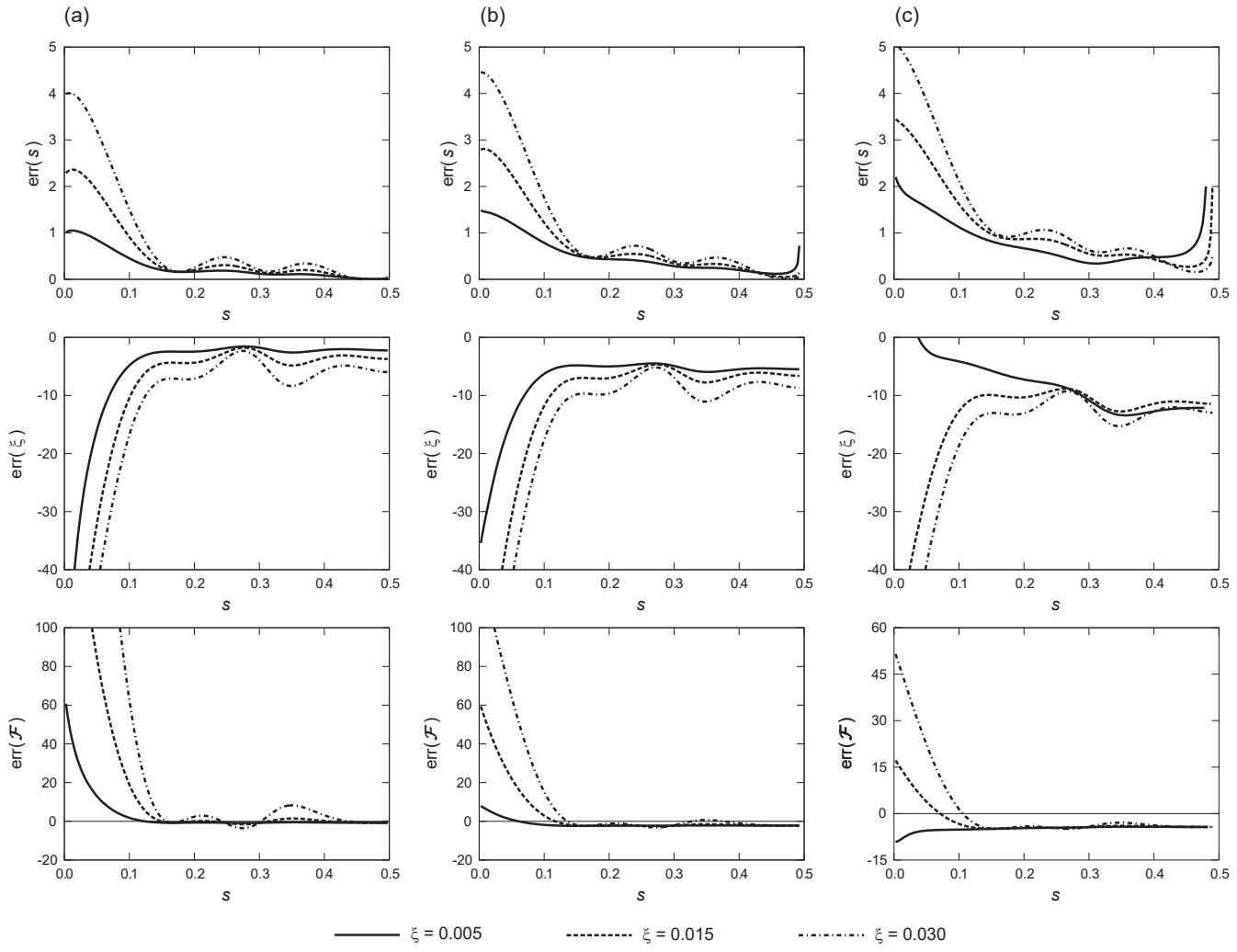

Figure 3: Elastically restrained cracked rod (4)–(8): identification using the variations of the first three eigenfrequencies of the longitudinal vibration. Values of $\mathcal{F}$: $\mathcal{F} = 5 \cdot 10^{-3}$ (left column), $\mathcal{F} = 15 \cdot 10^{-3}$ (central column), $\mathcal{F} = 30 \cdot 10^{-3}$ (right column). Percentage errors: $err(s) = 100 \times (s_{ident} - s_{exact})/\ell$, $err(\xi) = 100 \times (\xi_{ident} - \xi_{exact})/\xi_{exact}$, $err(\mathcal{F}) = 100 \times (\mathcal{F}_{ident} - \mathcal{F}_{exact})/\mathcal{F}_{exact}$.

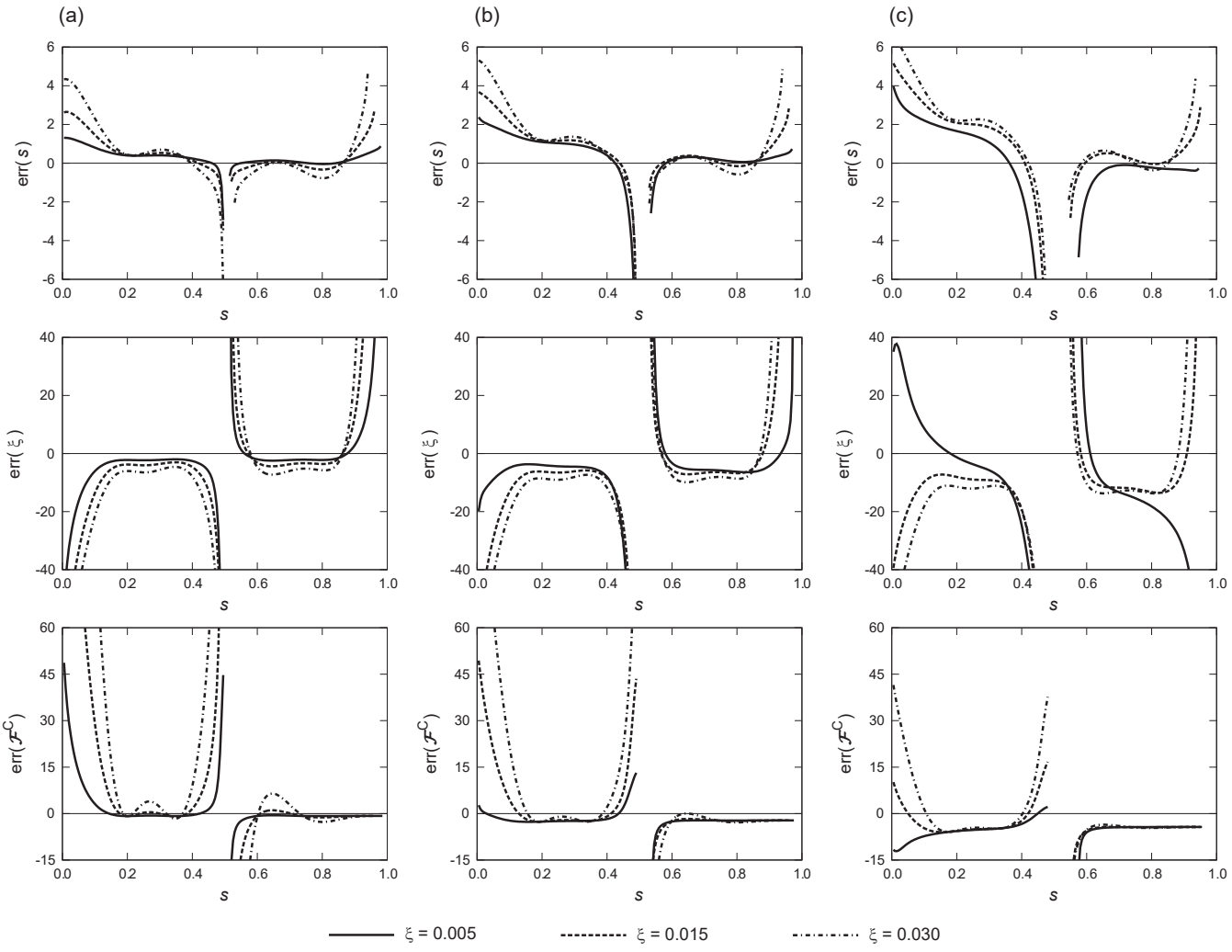

Figure 4: Elastically restrained cracked cantilever: identification using the variations of the first three eigenfrequencies of the longitudinal vibration. Values of $\mathcal{F}^C$: $\mathcal{F}^C = 5 \cdot 10^{-3}$ (left column), $\mathcal{F}^C = 15 \cdot 10^{-3}$ (central column), $\mathcal{F}^C = 30 \cdot 10^{-3}$ (right column). Percentage errors: $err(s) = 100 \times (s_{ident} - s_{exact})/\ell$, $err(\xi) = 100 \times (\xi_{ident} - \xi_{exact})/\xi_{exact}$, $err(\mathcal{F}^C) = 100 \times ({\mathcal{F}^C}_{ident} - {\mathcal{F}^C}_{exact})/{\mathcal{F}^C}_{exact}$.

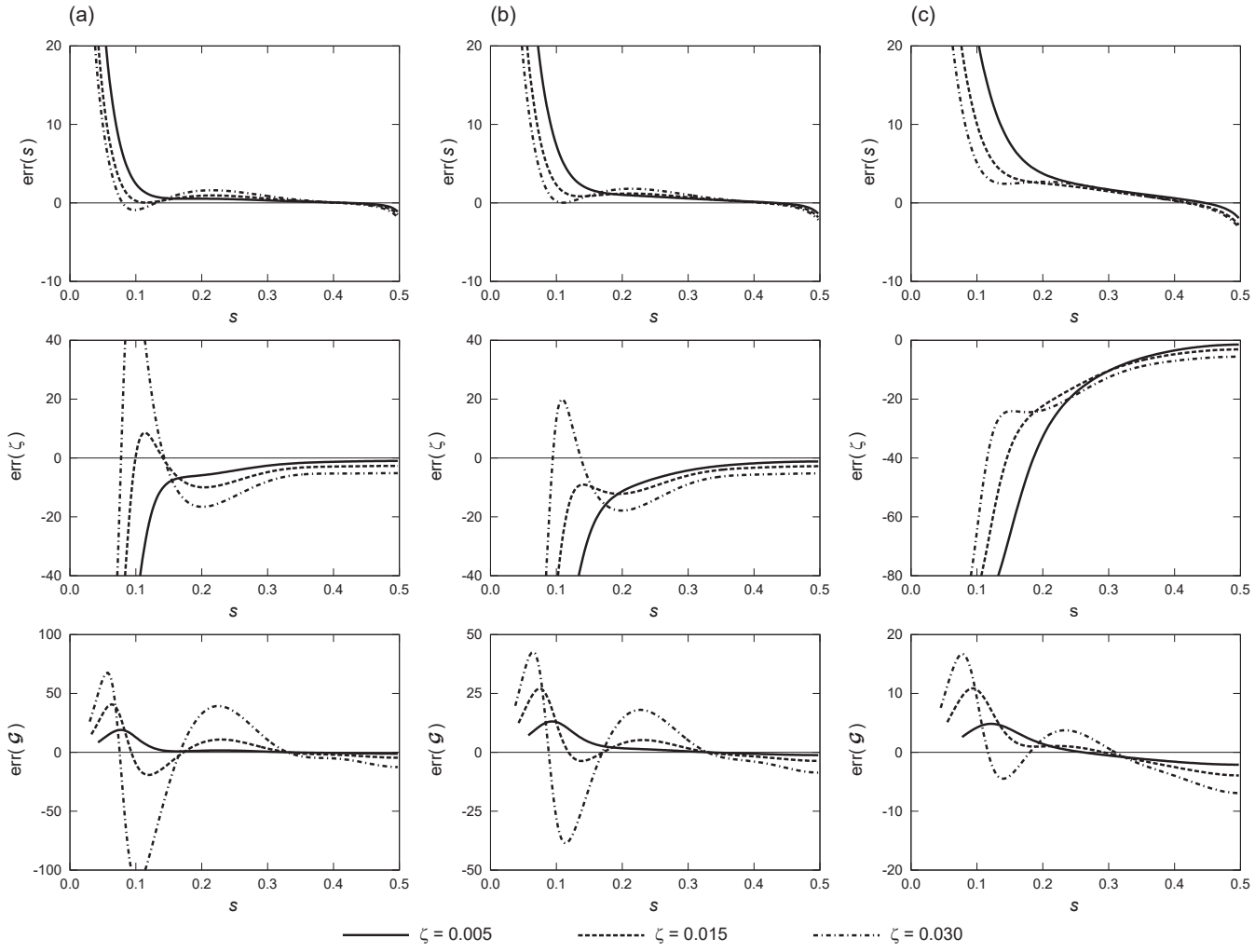

Figure 5: Elastically supported cracked beam (65)–(73): identification using the variations of the first three eigenfrequencies of the bending vibration. Values of $\mathcal{G}$: $\mathcal{G} = 1 \cdot 10^{-4}$ (left column), $\mathcal{G} = 2 \cdot 10^{-4}$ (central column), $\mathcal{G} = 6 \cdot 10^{-4}$ (right column). Percentage errors: $err(s) = 100 \times (s_{ident} - s_{exact})/\ell$, $err(\zeta) = 100 \times (\zeta_{ident} - \zeta_{exact})/\zeta_{exact}$, $err(\mathcal{G}) = 100 \times (\mathcal{G}_{ident} - \mathcal{G}_{exact})/\mathcal{G}_{exact}$.

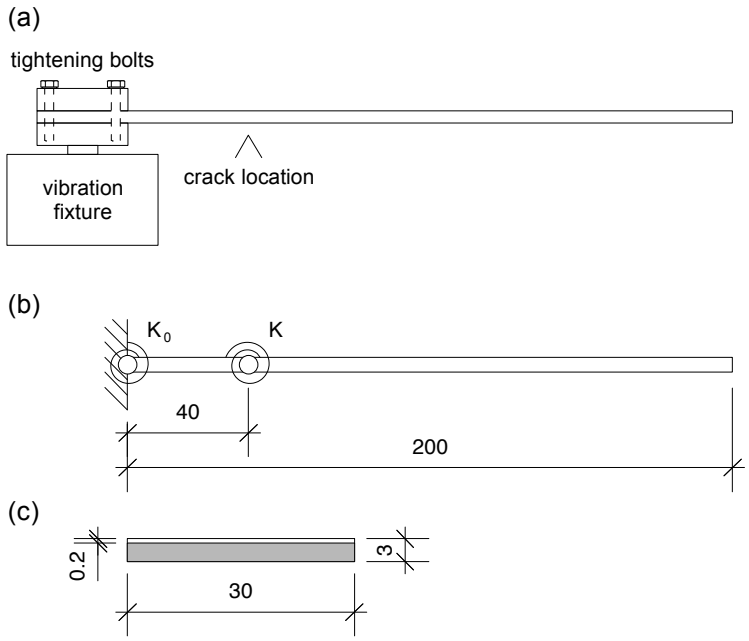

Figure 6: The cracked cantilever in bending vibration considered in [16]. (a) Schematic illustration of the experimental setup; (b) mechanical model; (c) cracked cross-section. Length in mm.

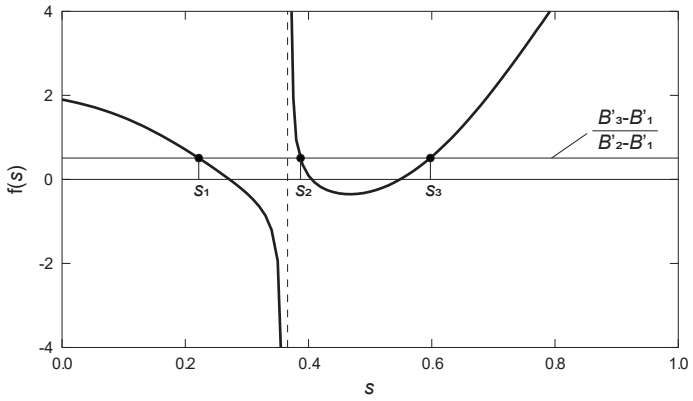

Figure 7: Results of damage identification for the cantilever in bending vibration. Actual damage location: $s = 0.20$.